This article has been accepted for publication in a future issue of this journal, but has not been fully edited. Content may change prior to final publication. Citation information: DOI 10.1109/TVT.2017.2779784, IEEE Transactions on Vehicular Technology

Optimal Power Scheduling for Uplink Transmissions in SIC-based Industrial Wireless Networks with Guaranteed Real-time Performance

Chaonong Xu, Kaichi Ma, Yida Xu, Yongjun Xu, and Yuguang Fang, *Fellow*, *IEEE*

***Abstract*—The k-SIC (Successive Interference Cancellation) technology can support at most k parallel transmissions, and thus fast media access can be provided, which is vital for real-time industrial wireless networks. However, it suffers from high power consumption because high interference caused by parallel transmissions has to be overcome. In this paper, given the real-time performance requirements, we consider a network supporting k-SIC, and study how to minimize aggregate power consumptions of user equipments for uplink transmissions by jointly addressing power allocation and user scheduling. We show that the problem is solvable in polynomial time in the case of continuous transmit powers by an algorithm with complexity of $O(nlog(n))$, where n is the number of user equipments. In the case of discrete transmit powers, the problem is shown to be polynomially solvable for 2-SIC, and we also propose an approximation algorithm for k-SIC where $k > 2$. Experimental evaluations reveal that the real-time performances have tremendous impacts on both the aggregate power consumption and the maximum of the transmit powers of user equipments. Besides, the usability of SIC in low-power applications is also shown by experimental evaluations.**

***Index Terms*—Successive Interference Cancellation, Uplink Scheduling, Power Control, Delay Guarantee, Energy Saving.**

I. Introduction

LOW delay guarantee is required in Ultra-Reliable and Low-Latency Communications (URLLC) in future Industrial Wireless Networks (IWNs) [1]. In many practical industrial monitoring systems, User Equipments (UEs) are deployed to sense environmental status and then feedback results to a Base Station (BS), where sensory data is aggregated. Since outdated sensory data is of no value for some time-sensitive applications such as real-time control or emergency alarm [2], the uplink transmission delay is an important performance metric for IWNs.

Time Division Multiple Access (TDMA) has the inherent advantage of bounded Media Access Control (MAC) delay. However, in TDMA systems, at most one transmitter is allowed to access wireless channel at any instant, thus the transmission delay could still be high if there are a large number of UEs. A new media access method is urgently needed for real-time IWNs.

Chaonong Xu, Kaichi Ma and Yida Xu are with Beijing Key Lab of Petroleum Data Mining, China University of Petroleum, Beijing, 102249, China (e-mail: xuchaonong@cup.edu.cn).

Yongjun Xu is with the Institute of Computing Technology, China Academy of Sciences, Beijing, 100190, China.

Yuguang Fang is with the Department of Electrical and Computer Engineering, University of Florida, Gainesville, FL, 32611, USA.

Supported by National Natural Science Foundation of China (61702487) and Science Foundation of China University of Petroleum, Beijing (ZX20150089).

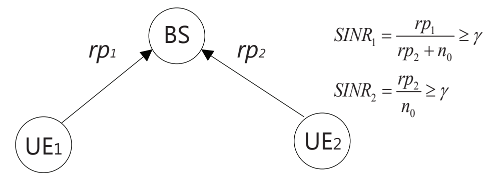

Fig. 1. Principle of SIC in uplink transmissions

In recent years, the Successive Interference Cancellation (SIC) technology has attracted interests of researchers from cellular networks. For example, the SIC technique has been used for multiuser multiplexing in power-domain Non-Orthogonal Multiple Access (NOMA) [3]. It is helpful for IWNs because it offers a possible way to meet stringent delay requirements by supporting Multi-Packet Reception (MPR), particularly when the number of UEs is large.

SIC technology supports MPR by exploiting the structure of the interference signals. In Fig.1, UE_1 and UE_2 transmit simultaneously to a BS, and their received powers at BS are rp_1 and rp_2, respectively. If $rp_1 > rp_2$ and the Signal-to-Interference-plus-Noise Ratio (SINR) of UE_1 is no less than γ, i.e., $SINR_1 \geq \gamma$, where γ is the decoding threshold, signal from UE_1 can be decoded successfully. Then, it is removed from the aggregate received signal, thus $SINR_2 = \frac{rp_2}{n_0}$. If $SINR_2 \geq \gamma$ holds, the signal from UE_2 can also be successfully decoded. Obviously, compared with the traditional TDMA, the channel access time based on the SIC technology is reduced by half in this example.

Although the SIC technology is valuable for real-time performance of IWNs, it suffers from high power consumption on the side of UEs for uplink transmissions. The reason is that the high interference caused by parallel transmissions has to be overcome by high transmit power in the SIC technology, which poses a serious challenge for the energy-constrained UEs [4].

We solve the problem by combining user scheduling and power allocation, or alternatively, power scheduling[1]. On one hand, the user scheduling determines how to group the UEs so that the UEs in a same group transmit simultaneously. On the other hand, the power allocation sets the transmit powers

[1]For convenience, in the rest of this paper, the term of joint power allocation and user scheduling is replaced with power scheduling.

This article has been accepted for publication in a future issue of this journal, but has not been fully edited. Content may change prior to final publication. Citation information: DOI 10.1109/TVT.2017.2779784, IEEE Transactions on Vehicular Technology

of UEs, so that all signals from the UEs in the same group can be decoded successfully. Therefore, it is naturally to find the optimal power scheduling strategy to minimize aggregated power consumption of UEs under given real-time performance guarantee, so that energy-constrained UEs can be utilized in IWNs.

In this paper, we first consider the problem with continuous transmit powers. By revealing the implication of a key term named Power Threshold Sequence (PTS), the original problem is converted to a user scheduling problem, based on the optimal solution to the problem of minimum power allocation in a toy network. In view of the conclusions obtained in the case, we further consider the same problem, however, with discrete transmit powers. We present an optimal algorithm for 2-SIC and an approximation algorithm for k-SIC where $k > 2$, respectively.

Our major contributions are summarized as follows. (1) We formulate the problem of minimizing aggregated power consumption for uplink transmissions in SIC-based real-time IWNs by combining user scheduling and power allocation. (2) We propose an optimal algorithm with complexity of $O(nlog(n))$ for the problem in the case of continuous transmit powers. (3) For the case with discrete transmit powers, we present an optimal algorithm with time complexity of $O(n^4)$ for 2-SIC. For k-SIC where $k > 2$, an approximation algorithm is presented. (4) We reveal the key insight on the tradeoff between the real-time performance and the power consumption, that is, the power consumption will be exponentially decreased with certain degradation of the real-time performance.

The remainder of this paper is organized as follows. Section II reviews the related works, and Section III elaborates the system model. The optimal power scheduling problem in the case of continuous transmit powers is discussed in Section IV. Based on the conclusions drawn in Section IV, the same problem in the case of discrete transmit powers is considered in Section V. Performance evaluation is carried out in Section VI, and the last section gives conclusions.

II. Related works

SIC has been intensively investigated because single-carrier NOMA is likely to be adopted as a standard for future 5G uplink transmissions. Therefore, we focus on related works in single-carrier wireless networks. As for SIC in multi-carrier communications, we refer readers to [4], [5] for an overview of SIC in 5G systems.

SIC can approach Shannon capacity under the assumption of perfect interference cancellation [6], therefore, it also attracts research interests in Wireless Local Area Networks (WLAN) and Wireless Personal Area Networks (WPAN) besides 5G networks in recent years [7]. Halperin et al. design a 2-SIC receiver for ZigBee [8]. Even without using any MAC scheme, it is reported that it could increase throughput by 1.8 times due to improved spatial reuse. Sen et al. suggest some potential techniques for designing SIC-aware scheduling algorithms [9].

To fully leverage the capability of SIC, cross-layer optimization frameworks aiming for higher performance are setup in [10]–[14]. Although [11] employs joint power allocation and link scheduling, it has different optimization target with ours. [11] is for Signal-to-Interference Ratio (SIR) balancing, and it is solved by maximizing the minimum SIR. Actually, it aims for throughput fairness at link layer. [13] is to maximize the minimum flow throughput at routing layer, and it is solved by the joint routing and link scheduling. Relatively, in this paper, we aim to minimize aggregate power consumption with guaranteed delay performances.

Scheduling without power allocation is also a research topic on SIC. Minimum length scheduling without power allocation is proved to be NP-hard in [15]. Lv et al. propose simultaneity graph to capture the characterisic of SIC [16], and Abishek et. al propose a distributed MAC protocol based on the k-SIC model [17].

Significant research works lay emphasis on downlink scheduling using SIC, including [4], [18], [19] and etc.. Distinct from them, the following papers focus on uplink transmissions based on SIC. Xu et al. propose a distributed uplink power allocation algorithm, which is to be used in random access for massive connections [14]. In [20], the complexities of uplink scheduling algorithms aiming for throughput and proportional fairness are studied, where the two problems are formulated with the received powers other than the transmit powers. In [21], a game-theoretic based distributed uplink power control algorithm is proposed for two interfering cells, the sum of powers will be minimized if some prerequisites are satisfied. Qian et al. take the component of dynamic base station association into consideration in uplink scheduling [22].

III. System Model

We consider a single-hop, single-channel wireless network consisting of n single-antenna UEs[2] $u_1, u_2, \ldots, u_n$, and a single-antenna base station. The base station is equipped with a k-SIC receiver. A k-SIC receiver can decode at most k signals at one time, provided that SINR of every signal after interference cancellation is higher than the decoding threshold of the receiver. We assume that the n UEs have data to transmit[3].

In the considered network, time is divided into frames, and a frame time is divided into multiple time slots. We assume that data packets generated by UEs have same size, both transmitting rate and sampling rate of UEs are fixed, and the time span of a slot is set for delivering a data packet. In fact, the above assumptions are tenable in reality [24].

We only consider perfect interference cancellation, i.e., the residual error is zero, which has been widely adopted.

The channel gain represents the loss of signal power as the signal propagates through the channel. We assume that the channel gain keeps constant during a frame time. Only in

[2] In this paper, UE, user and transmitter are used interchangeably, and receiver is equivalent to base station.

[3] At the beginning of a frame, these UEs which have transmission tasks will report themselves to base station via control channel. Since we only need to find the UEs which try to be transmitters of the upcoming frame, method such as [23], which is based on compressive sensing, can achieve the goal with low overhead.

This article has been accepted for publication in a future issue of this journal, but has not been fully edited. Content may change prior to final publication. Citation information: DOI 10.1109/TVT.2017.2779784, IEEE Transactions on Vehicular Technology

TABLE. I. Notations

S	user scheduling strategy
$S[i]$	ith slot of user scheduling strategy S
u_i	user equipment i
G_i	channel gain of u_i
L	frame length bound
$(\widehat{X}_1^{(r)}, \widehat{X}_2^{(r)}, \cdots, \widehat{X}_r^{(r)})$	power threshold sequence for r-SIC
γ	decoding threshold
n_0	power of noise
p_i	transmit power of u_i
$\widehat{tp}_i$	continuous transmit power of u_i in the optimal solution, where $i \in [1, k]$
$\widetilde{tp}_i$	discrete transmit power of u_i in the optimal solution, where $i \in [1, k]$
$\overline{TP} = \{\overline{tp}_m, \overline{tp}_{m-1}, \cdots, \overline{tp}_1\}$	feasible discrete transmit powers set
$[\![x]\!]$	$\underset{y \in \overline{TP} \bigcap (y \geq x)}{\arg\min} \quad (y - x)$
T_b	transmission delay bound
T_s	sampling cycle

the section of performance evaluation, we adopt the following channel gain model for wireless signal [25],

$$CG = -20log(f) - 26log(d) + 19.2,$$

where f is the frequency in Megahertz, and d is the Euclidean distance between the UE and the base station in meters. Using the channel gain model, we can obtain the channel gain of each UE based on its Euclidean distance with the base station.

Since our aim is to minimize the aggregate power consumption, the optimal transmit powers of UEs would not be very high. Therefore, we take no constraint of the maximal transmit power into consideration. In fact, the simplification results in the tractability of the problem.

IV. Real-time Minimum Power Scheduling for k-SIC

The problem of finding the minimum power scheduling strategy for uplink transmissions in SIC-based IWNs under guaranteed real-time performance is formally defined as follows.

Definition 1. Real-time Minimum Power Scheduling for k-SIC (RMPS-kSIC) Problem: Given a k-SIC receiver and n users $u_1, u_2, \cdots, u_n$ with channel gains $G_1, G_2, \cdots, G_n$, respectively. Without loss of generality (W.l.o.g.), we assume $G_1 \leq G_2 \leq \cdots \leq G_n$. At most k users can transmit simultaneously. Noise power is n_0 for all users. Let the transmit powers be $p_1, p_2, \ldots, p_n$, each of which is a continuous variable[4], such that the aggregate power consumption of the n users is minimized under the following constraints: (1) Every user is scheduled only once in a frame. (2) The frame length is not larger than the designated value L[5]. (3) SINR for every user is above the given decoding threshold γ.

Thus, RMPS-kSIC can be formulated as follows.

$$\min_{\{S, p_1, \ldots, p_n\}} \sum_{i=1}^{n} p_i \tag{1a}$$

$$s.t. \quad FL(S) \leq L \tag{1b}$$

$$0 \leq |S[j]| \leq k \quad j \in [1, L] \tag{1c}$$

$$\frac{G_i p_i}{I_i + n_0} \geq \gamma; \quad p_i \geq 0; \quad \forall i \in [1, n], \tag{1d}$$

where S represents the user scheduling strategy, $S[j]$ represents all users scheduled in the jth slot, and I_i is the power of interference when decoding signal of u_i. Apparently, the interference is only influenced by S if $\{p_1, p_2, \ldots, p_n\}$ are known. $FL(S)$ is the number of time slots in the scheduling strategy S, and L is the bound of frame length. Obviously, L should be at least $\lceil n/k \rceil$ for a k-SIC receiver. There may be multiple users scheduled in slot $S[j]$, $|S[j]|$ is thus the cardinality of $S[j]$.

RMPS-kSIC is a joint optimization of power allocation and user scheduling. Next, we show that based on the solution of the minimum power allocation problem for k-SIC in a toy network, RMPS-kSIC can be polynomially solved. Thus, we first define and solve the minimum power allocation problem for k-SIC in a toy network in subsection IV.A, and then introduce a polynomial-time algorithm to solve RMPS-kSIC in subsection IV.B.

A. Minimum power allocation for toy network

Definition 2. Minimal Power Allocation for r Parallel Transmitters (MPArPT): Given an uplink toy network consisting of a k-SIC receiver and r transmitters $u_1, u_2, \ldots, u_r$ with channel gains as $G_1, G_2, \ldots, G_r$, w.l.o.g., we assume $G_1 \leq G_2 \leq \ldots \leq G_r, r \leq k$, and n_0 is the noise power. Denote transmit powers of $u_1, u_2, \ldots, u_r$ by $p_1, p_2, \ldots, p_r$ respectively. Assign value for $p_1, p_2, \ldots, p_r$ so that the aggregate power consumption of the r users is minimized under the premise that $u_1, u_2, \ldots, u_r$ transmit simultaneously and their signals are all decoded successfully.

This problem is thus formulated as

$$\min_{\{p_1, \ldots, p_r\}} \sum_{i=1}^{r} p_i \tag{2a}$$

$$s.t. \quad \frac{G_i p_i}{I_i + n_0} \geq \gamma; \quad p_i \geq 0; \quad \forall i \in [1, r]. \tag{2b}$$

To solve MPArPT, we have to know the expression of I_i in the first step. Obviously, I_i is only dependent on the decoding order if $\{p_1, \ldots, p_r\}$ are known. Lemma 1 reveals that to achieve the optimal solution to MPArPT, the transmitters' signals must be decoded in the descending order of channel gains.

[4]In fact, there is no absolute continuous power variable. However, if the power levels are numerous enough and the power spacing is small enough, the output powers can be considered to be continuous.

[5]To achieve the guaranteed real-time performance, the time span of a frame must be no greater than half of the transmission delay bound. Their relationship will be revealed in detail in section VI.C.

This article has been accepted for publication in a future issue of this journal, but has not been fully edited. Content may change prior to final publication. Citation information: DOI 10.1109/TVT.2017.2779784, IEEE Transactions on Vehicular Technology

Lemma 1. If $\gamma > 1$, the optimal decoding order for MPArPT is the descending order of the channel gain of transmitters[6].

Proof. Please refer to Appendix.B.

Based on Lemma 1, MPArPT can be reformulated as follows.

$$\min_{\{p_1,\ldots,p_r\}} \sum_{i=1}^{r} p_i \tag{3a}$$

$$s.t. \quad \frac{G_l p_l}{\sum_{i=1}^{l-1} G_i p_i + n_0} \geq \gamma \quad l \in [2,r]; \quad \frac{G_1 p_1}{n_0} \geq \gamma; \tag{3b}$$

Definition 3. Power Threshold Sequence for r-SIC (r-PTS) is a sequence $\widehat{X} = \left(\widehat{X}_1, \widehat{X}_2, \ldots, \widehat{X}_r\right)$ which satisfies the following equality group

$$\begin{cases} \dfrac{\widehat{X}_l}{\sum_{i=1}^{l-1} \widehat{X}_i + n_0} = \gamma \quad \forall l \in [2,r] \\ \dfrac{\widehat{X}_1}{n_0} = \gamma \end{cases},$$

where $\widehat{X}_i > 0$ for all $i \in \{1,\ldots,r\}$.

Obviously, $\widehat{X}_r \geq \widehat{X}_{r-1} \geq \ldots \geq \widehat{X}_1$ if $\gamma > 1$, and $\widehat{X}_1 = \gamma n_0$, $\widehat{X}_{i+1} = (\gamma+1)\widehat{X}_i$ for $\forall i \in \{1,\ldots,r-1\}$. As shown in the following theorem, r-PTS is in fact the minimum received powers required for r signals if the r signals can be successfully decoded by a k-SIC receiver where $k \geq r$.

Theorem 1. For the following inequality group

$$\begin{cases} \dfrac{x_l}{\sum_{i=1}^{l-1} x_i + n_0} \geq \gamma \quad \forall l \in [2,r] \\ \dfrac{x_1}{n_0} \geq \gamma \end{cases} \tag{4}$$

, any of its solution $\left(\widetilde{X}_1, \widetilde{X}_2, \ldots, \widetilde{X}_r\right)$ satisfies $\widetilde{X}_i \geq \widehat{X}_i$ for $\forall i \in [1,r]$, where $\widehat{X} = \left(\widehat{X}_1, \widehat{X}_2, \ldots, \widehat{X}_r\right)$ is r-PTS.

Proof. Please refer to Appendix.C.

With Lemma 1 and Theorem 1, the optimal solution to MPArPT is shown in the following theorem.

Theorem 2. The optimal solution to MPArPT is $\left(\frac{\widehat{X}_1}{G_1}, \frac{\widehat{X}_2}{G_2}, \ldots, \frac{\widehat{X}_r}{G_r}\right)$.

Proof. Please refer to Appendix.D.

For convenience, $\frac{\widehat{X}_i}{G_i}$ is denoted as $\widehat{tp}_i$ in the following sections. Theorem 2 reveals that for user u_i with channel gain G_i, if its signal is to be decoded by a k-SIC receiver and its decoding order index is l where $l \leq k$, its transmit power should be at least $\frac{\widehat{X}_l}{G_i}$, which is the key to Algorithm 1 and Algorithm 2 in the following sections.

B. Solving RMPS-kSIC Problem

A key property of the optimal power scheduling strategy of RMPS-kSIC is shown in the following lemma.

[6]Since any signal could be decoded only if its power is greater than its interference power, $\gamma > 1$ is not a tight constraint in reality [26].

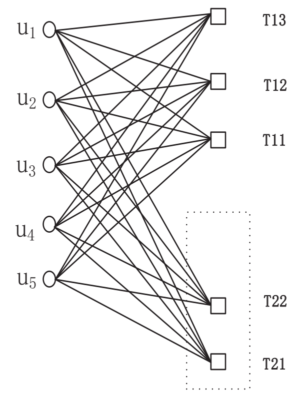

Fig. 2. An example of $GH(5,3,2)$ when $n = 5$, $k = 3$ and $L = 2$

Lemma 2. If $n \leq kL$, for the optimal power scheduling scheme of RMPS-kSIC, we have:

(1) The number of UEs scheduled in any slot is either $\lfloor n/L \rfloor$ or $\lceil n/L \rceil$.

(2) There are $L\lceil n/L \rceil - n$ slots, each of which is shared by $\lfloor n/L \rfloor$ UEs.

Proof. Please refer to Appendix.E.

Theorem 3. For a network of n users and two integers k_1 and k_2, if $L \geq n/min(k_1,k_2)$, the optimal power scheduling strategy of RMPS-k_1SIC is the same as that of RMPS-k_2SIC.

Proof. Based on Lemma 2, the optimal power scheduling strategy for RMPS-k_1SIC problem is a feasible solution to RMPS-k_2SIC, and vice versa. So, the two optimal power scheduling strategies are the same. □

Theorem 3 shows that if $n \leq kL$, the optimal power scheduling strategy is only related to L rather than k.

Based on the definition of PTS and Theorem 2, we develop an algorithm for the optimal solution to the RMPS-kSIC problem, which converts RMPS-kSIC into the problem of finding a Maximum Weight Matching (MWM) of a balanced complete bipartite graph.

Algorithm 1. Optimal algorithm for the RMPS-kSIC problem {
1. $GH(n,k,L)$=ϕ; Compute k-PTS as $(\widehat{X}_1, \widehat{X}_2, \ldots, \widehat{X}_k)$.
2. add n graph nodes with label u_i where $i \in [1,n]$ into $GH(n,k,L)$; // part I of the graph
3. add $L\lfloor n/L \rfloor$ graph nodes with label T_{hj} where $h \in [1,L]$ and $j \in [1, \lfloor n/L \rfloor]$ into $GH(n,k,L)$; $M = \widehat{X}_k/G_1$;
4. if($n\%L$!=0){
5. for(i=1; $i \leq n\%L$; i++) add a graph node with label $T_{i\lceil n/L \rceil}$ into $GH(n,k,L)$; } //part II of the graph
6. for any graph node u_i {
7. for any graph node T_{hj} {
8. add an edge (u_i, T_{hj}) with weight $-\widehat{X}_j/G_i + M$;}}
9. find an MWM of the complete bipartite graph;
10. for any (u_i, T_{hj}) in the MWM, u_i will be scheduled in the hth slot with power $\widehat{X}_j/G_i$;}

Line 2 to line 8 in Algorithm 1 generates a balanced complete bipartite graph $GH(n,k,L)$, where nodes in part I of the bipartite graph correspond to the set of the n UEs,

This article has been accepted for publication in a future issue of this journal, but has not been fully edited. Content may change prior to final publication. Citation information: DOI 10.1109/TVT.2017.2779784, IEEE Transactions on Vehicular Technology

and these in part II correspond to the set of decoding indices in spatial-temporal dimension. Furthermore, the edge (u_i, T_{hj}) means that u_i can be scheduled in the hth slot, and its decoding order index at base station is j. In other words, an edge of the graph specifies a scheduling-decoding arrangement for a UE[7]. Obviously, all possible scheduling-decoding arrangments for the n UEs are revealed by the complete bipartite graph. For the edge (u_i, T_{hj}), since its weight is the sum number of the inverse of the minimal transmit power of u_i required for the scheduling-decoding phase plus a sufficient large number M, the MWM of $GH(n, k, L)$ corresponds to a feasible power scheduling strategy.

We give an example of $GH(5, 3, 2)$ in Fig.2, where the weights of edges are omitted for clarity.

The following result shows that the power scheduling strategy mapped from the MWM is the optimal.

Theorem 4. Algorithm 1 outputs an optimal solution to the RMPS-kSIC problem.

Proof. Please refer to Appendix.F.

In fact, it is PTS that decouples power allocation and user scheduling in RMPS-kSIC without impairing the optimality. Thus, PTS is a fundamental item which provides key insights into the algorithm.

If the MWM is found by Kuhn-Munkres algorithm, the time complexity of Algorithm 1 will be $O(n^3)$ since that of Kuhn-Munkres algorithm is $O(n^3)$. A faster algorithm is possible since $GH(n, k, L)$ is a balanced complete bipartite graph, which is presented as follows.

Algorithm 2. A faster algorithm for the RMPS-kSIC problem {

OUT=ϕ.

sort $u_1, u_2, \ldots, u_n$ in the ascending order of their channel gains, w.l.o.g., assume $G_1 \leq G_2 \leq \ldots \leq G_n$;

for(i=1;$i \leq \lfloor \frac{n}{L} \rfloor$;$i$++){

  for(j=1;$j < L+1$;j++){

    add edge $(u_{(i-1)L+j}, T_{ji})$ into OUT;}}

for(i=1;$i \leq n\%L$;i++){

  add edge $(u_{n-i+1}, T_{i\lceil \frac{n}{L} \rceil})$ into OUT;}

Theorem 5. Algorithm 2 outputs the optimal solution to the RMPS-kSIC problem.

Proof. Please refer to Appendix.G.

The complexity of Algorithm 2 is determined by the sorting algorithm used. It is $O(nlogn)$ if the classic quick sorting algorithm is adopted. Based on the complexity comparison between Algorithm 2 and Algorithm 1, for our problem, Algorithm 2 is obviously better.

V. The Minimum Discrete Power Scheduling for k-SIC

Assume there are m transmit power levels $\overline{tp}_m, \overline{tp}_{m-1}, \ldots, \overline{tp}_1$ where $\overline{tp}_m > \overline{tp}_{m-1} > \ldots > \overline{tp}_1$, and they form a feasible power set $\overline{TP} = \{\overline{tp}_m, \overline{tp}_{m-1}, \ldots, \overline{tp}_1\}$. The Real-time Minimum Discrete Power Scheduling for k-SIC (RMDPS-kSIC) problem is formulated as follows.

$$\min_{\{S, p_1, \ldots, p_n\}} \sum_{i=1}^{n} p_i \tag{5a}$$

$$s.t. \quad p_i \in \overline{TP} \quad for \quad \forall i \in [1, n]; \tag{5b}$$

$$(1b); \qquad (1c); \qquad (1d). \tag{5c}$$

In the following subsections, we solve RMDPS-kSIC problem for $k = 2$ and $k > 2$, respectively.

A. Minimum discrete power scheduling for 2-SIC

Define $TP(i,j) = \left[\!\left[\frac{\widehat{X}_1}{G_i} \right]\!\right] + \left[\!\left[\frac{\gamma \left[\!\left[\frac{\widehat{X}_1}{G_i} \right]\!\right] G_i + \widehat{X}_1}{G_j} \right]\!\right]$, where $[\![x]\!] = \arg\min_{(y \in \overline{TP}) \cap (y \geq x)} (y - x), (x > 0)$. In other words, $[\![x]\!]$ is an item that satisfies: (1) It belongs to the set $\overline{TP}$; (2) It is not less than x and the nearest to x. In fact, $TP(i,j)$ is the minimum discrete transmit powers sum of UE_i and UE_j, if they transmit simultaneously and the signal of UE_i is decoded before that of UE_j.

Algorithm 3 solves RMDPS-2SIC problem.

Algorithm 3. An optimal algorithm for RMDPS-2SIC {

1. construct graph GH including n real graph nodes with label $u_1, u_2, \ldots, u_n$, and $2L - n$ virtual graph nodes with label $v_1, v_2, \ldots, v_{2L-n}$; $M = 2\overline{tp}_m$;
2. for any two real graph nodes u_i and u_j{
3.   if $(TP(i,j) < TP(j,i))$ the weight of their connecting edge is set as $-TP(i,j) + M$; else set it as $-TP(j,i) + M$;}
4. for any real graph node u_i and any virtual node {
5.   the weight of their connecting edge is set as $-\left[\!\left[\frac{\widehat{X}_1}{G_i} \right]\!\right] + M$; }
6. find an $MWM(GH)$ using Edmond′s blossom algorithm[8]; //setting transmit power based on $MWM(GH)$
7. for every matching edge in $MWM(GH)$ denoted as (i, j) {
8.   switch (type of i, type of j) {
9.   case (both i and j are real graph nodes) : {
10.   if $(TP(i,j) < TP(j,i))$
11. (p_i, p_j)=$\left(\left[\!\left[\frac{\widehat{X}_1}{G_i} \right]\!\right], \left[\!\left[\frac{\gamma \left[\!\left[\frac{\widehat{X}_1}{G_i} \right]\!\right] G_i + \widehat{X}_1}{G_j} \right]\!\right] \right)$;
12.   else (p_i, p_j)=$\left(\left[\!\left[\frac{\gamma \left[\!\left[\frac{\widehat{X}_1}{G_j} \right]\!\right] G_j + \widehat{X}_1}{G_i} \right]\!\right], \left[\!\left[\frac{\widehat{X}_1}{G_j} \right]\!\right] \right)$;
13. u_i and u_j share a time slot; break;}
14.   case (i is real node, j is virtual node) : {p_i=$\left[\!\left[\frac{\widehat{X}_1}{G_i} \right]\!\right]$; u_i exclusively occupies a time slot;break; }
15.   case else: *break*; //this case could not be executed
16.   end case }}

The idea of Algorithm 3 is similar to that of Algorithm 1. From line 1 to line 5, the graph GH is set up, where the n real graph nodes correspond to the n UEs, while the $2L - n$ virtual graph nodes are set up intentionally to ensure that the cardinality of $MWM(GH)$ is at most L, which will be proved in Theorem 6. Furthermore, the meaning of the edge connecting two real graph nodes is that the two corresponding UEs can be scheduled simultaneously, and its weight is equal

[7]More formally, the scheduling-decoding arrangement is also called the scheduling-decoding phase in this paper.

[8]Edmond′s blossom algorithm is a universal algorithm for finding an MWM of a general graph, while Kuhn-Munkres algorithm is only suitable for a bipartite graph.

This article has been accepted for publication in a future issue of this journal, but has not been fully edited. Content may change prior to final publication. Citation information: DOI 10.1109/TVT.2017.2779784, IEEE Transactions on Vehicular Technology

to the reverse of their mininal aggregate transmit powers plus a sufficient large number M. For the edge connecting a real graph node and a virtual graph node, it means that the UE corresponding to the real graph node monopolizes a slot, and the weight of the edge is equal to the reverse of their minimal aggregate transmit powers for correct decoding plus M. In line 6, $MWM(GH)$ is found, and from line 7 to the last line of Algorithm 3, the transmit powers of all UEs are set by checking every edge of the MWM sequentially.

Theorem 6. Algorithm 3 solves RMDPS-2SIC, if $\overline{tp}_m \geq \max\limits_{(\forall i,j\in[1,n])\cap(i\neq j)} \max\left\{ \left[\!\!\left[\frac{\gamma\left[\!\left[\frac{\widehat{X}_1}{G_i}\right]\!\right]G_i+\widehat{X}_1}{G_j}\right]\!\!\right], \left[\!\!\left[\frac{\gamma\left[\!\left[\frac{\widehat{X}_1}{G_j}\right]\!\right]G_j+\widehat{X}_1}{G_i}\right]\!\!\right] \right\}$.

Proof. Please refer to Appendix.H.

The time complexity of Algorithm 3 is determined by that of the Edmond's blossom algorithm, which is $O(n^4)$.

B. Minimum discrete power scheduling for k-SIC

Similar to Algorithm 3, we present an approximation algorithm for RMDPS-kSIC.

Algorithm 4. An approximation algorithm for RMDPS-kSIC {
1. using Algorithm 1 to compute an optimal user scheduling strategy S for RMPS-kSIC;
2. for every slot i in S {
3. sort UEs in $S[i]$ such that $G_{(S[i][j])} \leq G_{(S[i][j+1])}$ for $\forall j \in [1, |S[i]|-1]$.
4. $\widetilde{tp}_{[i][1]}=\left[\!\!\left[\frac{\widehat{X}_1}{G_{S[i][1]}}\right]\!\!\right]$;
5. for ($h = 2$; $h \leq |S[i]|$; h++) {
6. $\widetilde{tp}_{[i][h]}=\left[\!\!\left[\frac{\gamma}{G_{S[i][h]}}\left(n_0+\sum\limits_{j=1}^{h-1}\widetilde{tp}_{[i][j]}G_{S[i][j]}\right)\right]\!\!\right]$;}}}

A simple explanation of Algorithm 4 is as follows. First, a user scheduling scheme S is obtained by Algorithm 1. Then, for the $|(S[i])|$ users in slot i of S, the transmit power of the UE with the smallest channel gain in the slot is set based on $\widehat{X}_1$. In the last, the transmit power of the next UE is set greedily as the minimum discrete power for successful decoding. Obviously, if $\overline{tp}_m \geq \max\{\widetilde{tp}_{[1][|S[1]|]}, \widetilde{tp}_{[2][|S[2]|]}, \ldots, \widetilde{tp}_{[L][|S[L]|]}\}$, the power scheduling strategy generated by Algorithm 4 is feasible. Besides, the complexity of this algorithm is $O(n^2)$. However, although algorithm 4 has low time complexity, it is an approximation algorithm, which means that it may output a suboptimal solution.

Theorem 7 below reveals the approximation ratio of Algorithm 4 if $\frac{\overline{tp}_{i+1}}{\overline{tp}_i}$=$\rho > 1$ for $\forall i \in [1, m-1]$, i.e., when the ratio of two successive digital transmit powers is fixed.

Lemma 3. $\widehat{tp}_i = \frac{1}{G_i}\left(G_1\widehat{tp}_1 + \gamma\sum\limits_{j=1}^{i-1}\widehat{tp}_jG_j\right)$ for $\forall i \in [2, k]$, where $\widehat{tp}_1 = \frac{\widehat{X}_1}{G_1}$, and $(\widehat{X}_1, \widehat{X}_2, \ldots, \widehat{X}_k)$ is k-PTS.

Proof. Since $\left(\widehat{tp}_1, \widehat{tp}_2, \ldots, \widehat{tp}_k\right)$ is the optimal solution to MPAkPT problem, we therefore have $\frac{\widehat{tp}_iG_i}{n_0+\sum\limits_{j=1}^{i-1}\widehat{tp}_jG_j} = \gamma$. So,

$$\widehat{tp}_i = \frac{1}{G_i}\left(G_1\widehat{tp}_1 + \gamma\sum_{j=1}^{i-1}\widehat{tp}_jG_j\right). \quad \square$$

Theorem 7. For the feasible power set $\overline{TP} = \{\overline{tp}_m, \overline{tp}_{m-1}, \ldots, \overline{tp}_1\}$, where $\frac{\overline{tp}_{i+1}}{\overline{tp}_i} = \rho > 1$ for $\forall i \in [1, m-1]$, if $\overline{tp}_m$ is no less than the maximum of the transmit powers allocated to UEs by Algorithm 4, the approximation ratio of Algorithm 4 is no more than

$$\max\left\{ \begin{array}{l} \rho^{\lfloor\frac{n}{L}\rfloor}\left(\max\limits_{i\in[(n\%L)+1,L]}\frac{G_{i+(\lfloor\frac{n}{L}\rfloor-1)L}}{G_i}\right)^{\lfloor\frac{n}{L}\rfloor-1}, \\ \rho^{\lceil\frac{n}{L}\rceil}\left(\max\limits_{i\in[1,n\%L]}\frac{G_{i+\lfloor\frac{n}{L}\rfloor L}}{G_i}\right)^{\lfloor\frac{n}{L}\rfloor} \end{array} \right\}.$$

Proof. Please refer to Appendix.I.

As for the assumption in Theorem 7, i.e., $\overline{tp}_m$ must be no less than the maximum of the transmit powers allocated to UEs by Algorithm 4, it is not strict in reality due to the following two reasons. (1) k is usually a small integer for k-SIC receiver, therefore the assumption can be easily satisfied. (2) The maximum of the transmit powers decreases exponentially with the degradation of real-time performance, which will be observed in the performance evaluation section. Therefore, even if the assumption in Theorem 7 does not hold, a slight degradation of the real-time performance will meet the assumption.

VI. Performance Evaluation

We conduct a series of simulation experiments to demonstrate the effectiveness of the algorithms presented in this paper. The simulation parameters are as follows. The noise power spectral density is -169dBm/Hz, and the channel bandwidth is 200kHz, thus n_0 is -116dBm. The frequency spectrum is around 2.4GHz, and the decoding threshold γ is 2. The regular transceiver that does not support SIC is represented by k=1. We have not bounded $\overline{tp}_m$ which is the maximal discrete transmit power. The minimal discrete transmit power $\overline{tp}_1$ is -25dBm, and ρ is 3dB.

Since we are concerned with power consumption, we use the sum of the transmit powers of all transmitters as the performance metric for power consumptions.

A wireless network consisting of 30 UEs and one base station is constructed, where the base station is situated at the center of a square with sides of 120 meters, and all UEs are placed uniformly in the square.

A. Power consumption with real-time performance

Based on Lemma 2, if the given real-time performance is tighter, i.e., the frame length is smaller, the aggregate power consumption will be larger. In our experiments, we set the value of k as 1, 2, 3, 4, 5, and the frame length is from $\lceil 30/k \rceil$ to 35, i.e., the real-time performance requirement varies from the tightest to the loosest.

Just as what illustrated by Fig.3, for equal frame lengths, the aggregate power consumption is not affected by k. The fact is consistent with Theorem 3.

The case where $n = kL$ is termed as FSC (Full Slots Case) for convenience. Starting from FSCs, the aggregate power consumption decreases exponentially with increasing frame length. From Fig.3, we find that the aggregate power

This article has been accepted for publication in a future issue of this journal, but has not been fully edited. Content may change prior to final publication. Citation information: DOI 10.1109/TVT.2017.2779784, IEEE Transactions on Vehicular Technology

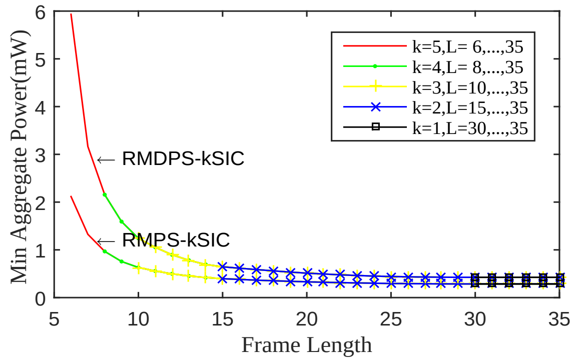

Fig. 3. Aggregate power consumption with real-time performance

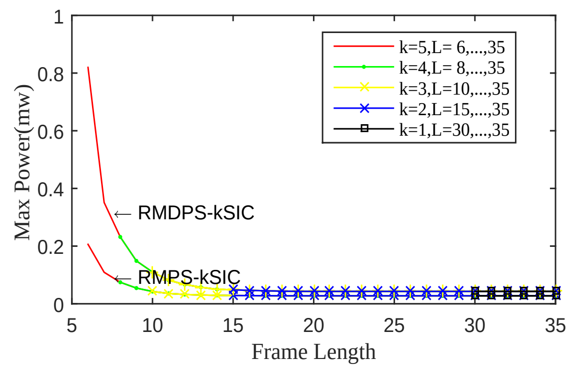

Fig. 4. Maximum of the transmit powers among UEs with real-time performance

consumption is 1.3mW when k=5 and L=7, while it is 2.1mW when k=5 and L=6. In other words, the power saving is prominent near the FSCs. However, it will diminish fast if the frame length continues to increase.

With different values of k and L, the maximum of the transmit powers among the 30 UEs are illustrated in Fig.4. Obviously, for all FSCs, the smaller the k, the less the maximum. Besides, similar to the aggregate power consumption, if the frame lengths are the same, the maximum of the transmit powers are also the same, and have no relation to k if $n \leq kL$. It also decreases exponentially if the real-time performance is even slightly relaxed from the FSCs. Take for example $k = 5$ and $L = 6$, which is an FSC, the maximum is $0.21mW$. If $k = 5$ and $L = 7$, it is only $0.11mW$. The maximum will decrease exponentially if the frame length continues to increase. All of these facts are consistent with Theorem 3.

The results of the above experiments reveal that relative to the number of parallel transmitters supported by the SIC receiver, the real-time performance requirement has tremendous impacts on both the aggregate power consumption and the maximum of the transmit powers. Besides, starting from the FSC, both the aggregate power consumption and the maximum of the transmit powers will exponentially decrease with the degradation of the real-time performance requirement.

For typical values of k, we note that the maximum of the transmit powers is acceptable. For example, if $k = 3$, the maximum is only 0.04mW, and it is 0.07mW if k=4, which are completely acceptable in practice even for low-power RF chips. In other words, with the optimal power scheduling strategy, SIC technology is suitable for low-power UEs.

B. Distribution of power consumptions

Based on Theorem 2, we know that the optimal transmit power is $\left(\frac{\widehat{X}_1}{G_1}, \frac{\widehat{X}_2}{G_2}, \ldots, \frac{\widehat{X}_r}{G_r}\right)$ for MPArPT. Since $\widehat{X}_1 \leq \widehat{X}_2 \leq \ldots \leq \widehat{X}_r$ and $G_1 \leq G_2 \leq \ldots \leq G_r$, the transmit powers of r UEs may be close to each other, i.e., the power consumptions may be balanced. Since the power balance brings long lifetime of networks, which is especially important for mobile applications.

We plot the distributions of transmit powers in Fig.5. Since we only care about deviations of transmit powers rather than transmit powers, for every experiment, we plot $\{x_1 - x_{min}, x_2 - x_{min}, \ldots, x_{30} - x_{min}\}$ using boxplot in Matlab, where $x_{min} = \min\{x_1, x_2, \ldots, x_{30}\}$. For clear comparison, the distributions of both RMPS-kSIC and RMDPS-kSIC are illustrated[9].

From Fig.5, we observe that the transmit power distributions are more and more imbalanced with the increasing k near FSCs. Take the FSCs in RMPS-kSIC for example, the biggest deviation of transmit powers are $0.028mW$, $0.038mW$ and $0.058mW$ for k=2, 3, 4, respectively. The cause of the imbalance is that a larger k naturally brings in larger transmit power near FSCs. The reason of the aggravating imbalance with increasing k is as follows. Because $\{\widehat{X}_1, \widehat{X}_2, \ldots, \widehat{X}_k\}$ is a geometric sequence, $\widehat{X}_k$ increases rapidly with increasing k, which results in the increment of the maximal transmit power.

For these cases where $L \geq 15$, power deviations are all the same whatever k is. The reason is that all optimal power scheduling strategies are the same for k=2, 3 and 4. Besides, for any given k, the mean power deviation is generally not increasing with the increasing L. The fact is inevitable because the transmit powers will decrease with relaxed real-time performance requirement.

The transmit power distributions in RMDPS-kSIC for k=2, 3, 4 have similar conclusions to those in RMPS-kSIC, although they are more imbalanced relative to those in RMPS-kSIC. We take the special case of L=23 for example, the mean power deviation in RMDPS-3SIC is $0.01mW$, while it is $0.009mW$ in RMPS-3SIC. Obviously, the gap is caused by the discontinuity of the discrete transmit powers.

For both RMPS-kSIC and RMDPS-kSIC, neither the maximum nor the median of the transmit powers grows with the increasing frame length. The reason is as follows. With the increment of frame length, the number of scheduling-decoding phases also increases. Therefore, more scheduling-decoding phases are provided besides these obtained using smaller frame length, which results in the non-increments of both the maximum and the median of the transmit powers.

[9]In every subgraph of Fig.5, the two black bar represent the maximum and the minimum, respectively, the blue box represents the region between the upper quartile and the lower quartile, and the red bar represents the median.

This article has been accepted for publication in a future issue of this journal, but has not been fully edited. Content may change prior to final publication. Citation information: DOI 10.1109/TVT.2017.2779784, IEEE Transactions on Vehicular Technology

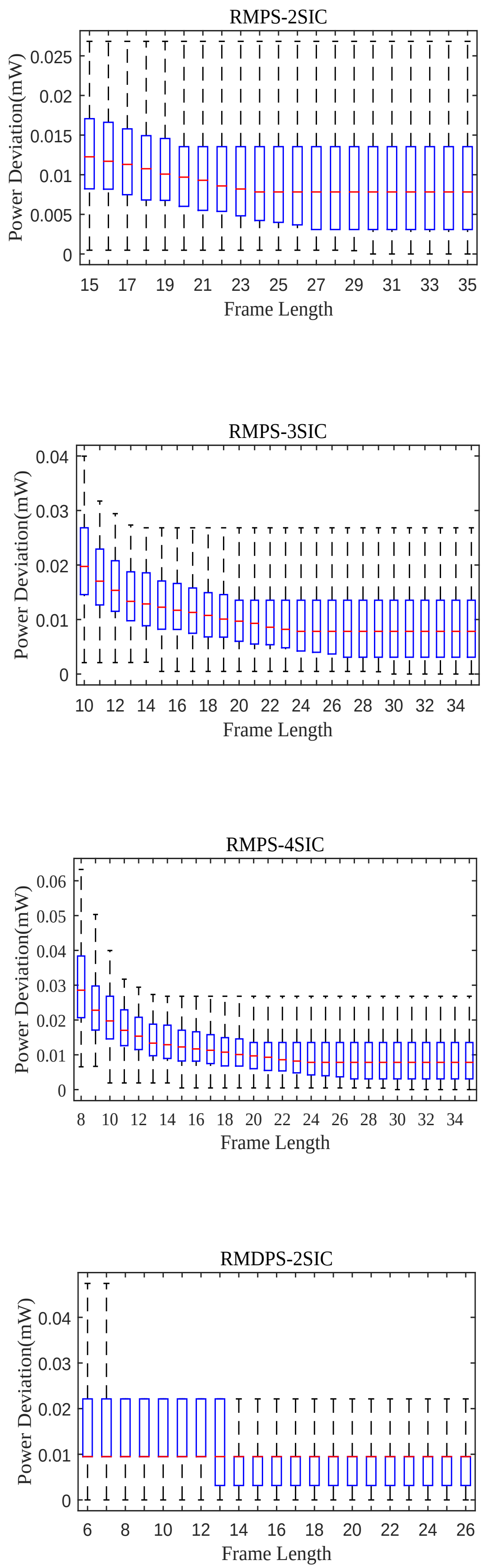

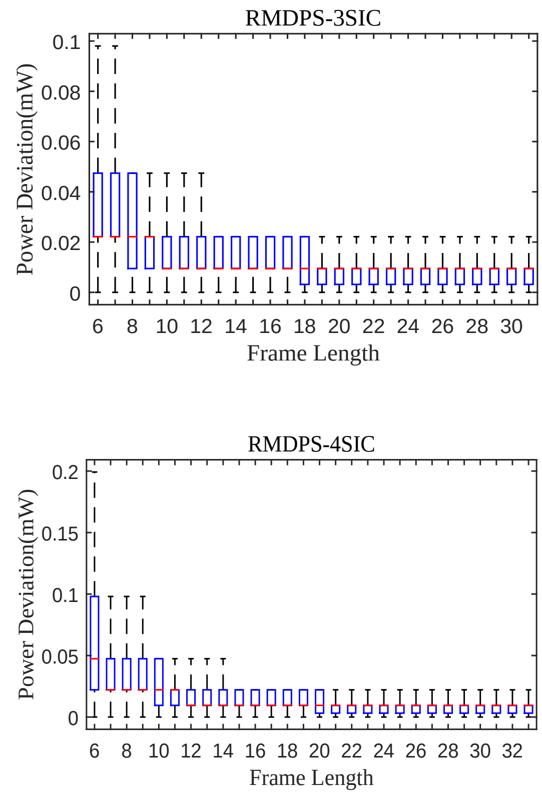

Fig. 5. Transmit power distributions of RMPS-kSIC and RMDPS-kSIC

C. Real-time performance

Using the time span of a slot as the basic time unit, we assume that the sampling cycle of all UEs are same, and the sampling cycle is denoted by T_s. The maximal delay bound is assumed to be T_b, which is the real-time performance bound, and the number of UEs is n.

Obviously, only if $2L \leq T_b \leq T_s$ holds, the real-time performance will be guaranteed. Therefore, $\lfloor T_b/2 \rfloor$ is the maximal value for L to guarantee the delay performance. Based on Lemma 2, if k is no less than $\lceil n/L \rceil$, every UE will be given a transmitting opportunity in a frame. Therefore, for any packet of any UE, the delay time is no more than T_b, i.e., the real-time performance is guaranteed.

The above method may result in so large value of k that it is not acceptable in reality. However, the value of k could be smaller if we know the specific number of transmitters, which is denoted by $\hat{n}$, at the beginning of a frame. In that case, if $k \geq \lceil \hat{n}/L \rceil$, the real-time performance can still be satisfied.

The following experiment is done to verify the real-time performance using the default network parameters. Other parameters settings specific to the experiment are as follows, T_b=12, T_s=18, L=6, and the sampling times of the 30 UEs start uniformly in $[0, 17]$. According to above analysis, if $k \geq 3$, no transmission delay[10] will be statistically larger than T_b. Otherwise, the real-time performance will not be

[10]The transmission delay of a packet is the time span from the birth of the packet to its being received by the base station.

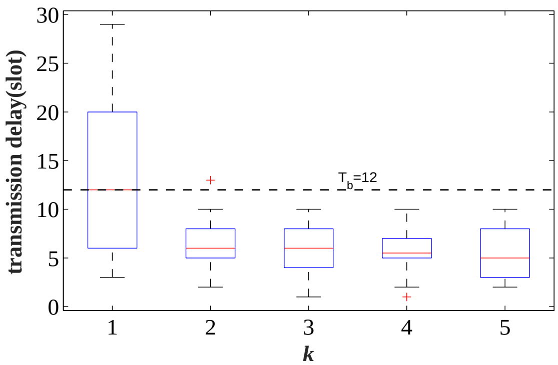

Fig. 6. Real-time performance with k

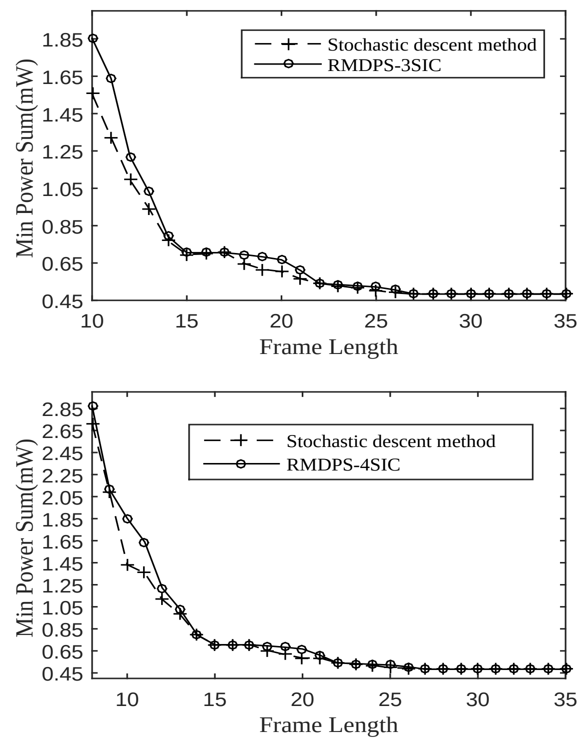

Fig. 7. Performance comparison between RMDPS-kSIC and stochastic descent method

guaranteed, although most of the transmission delays are less than T_b. The statistics of the transmission delays of all UEs are illustrated in Fig.6[11], where the x-axis is k, and the y-axis is the transmission delay.

From Fig.6, we can see that, almost half of the packets have delay larger than T_b when $k = 1$, only one packet has delay larger than T_b when $k = 2$, and all packet delays are less than T_b when $k \geq 3$. Obviously, they are consistent with our expectations, since the smaller k means the less throughput, which results in extra buffering delays of data packets.

We have some discussions on the number of UEs, i.e., n, in the following. Actually, it is closely related with k, T_s and T_b. In the worst case, i.e., $T_s = T_b$, only if $n \leq k\lfloor T_b/2 \rfloor$, the delay performance can be guaranteed. If $T_s > T_b$, n can be larger because less UEs simultaneously request transmission. Take the case of this experiment for example, if the sampling times start uniformly in $[0, T_s - 1]$ and $n \leq kT_s$, the delay performance can also be guaranteed. The conclusion is obviously verified in Fig.6.

D. Approximation ratio

Theorem 7 only reveals a performance lower bound of Algorithm 4, which is somehow pessimistic. To have an objective evaluation for Algorithm 4, the optimal solution to RMDPS-kSIC has to be found. However, finding the optimal solution is very hard for $k > 2$. Therefore, we find a suboptimal solution to RMDPS-kSIC using a heuristic algorithm, and then compare its aggregate power consumption performance with that by Algorithm 4.

The heuristic algorithm is in fact a stochastic descent algorithm: for a given user scheduling strategy, we first compute the optimal power consumption of the given strategy, which is the sum of the minimum power consumption in every time slot. The minimum power consumption in any time slot can be known by a simple brute-force search. Second, we randomly choose two transmitters and exchange their positions in the scheduling strategy, and then compute the minimum power consumption of the newly generated schedule strategy. If it is lower, the newly generated user scheduling strategy is accepted, otherwise it is discarded. The process continues iteratively until the aggregate power consumption is convergent.

[11]Note the experiment results have no relations with the power scheduling algorithm adopted, because algorithms in this paper are to generate an eligible power scheduling strategy with the minimum aggregate power consumption instead of delay.

Since the initial user scheduling strategy for iterations in the stochastic descent algorithm is the output of Algorithm 4, the suboptimal strategy generated by the stochastic descent algorithm always has less power consumption than that by Algorithm 4. Experimental results are illustrated in Fig.7 for k=3 and k=4. From Fig.7, we find that the minimum aggregate power consumption of Algorithm 4 is very close to that of stochastic descent algorithm. In other words, Algorithm 4 is virtually highly efficient.

E. Power consumption with decoding threshold and noise

With the same network as that in previous subsections, we try to reveal the relationships among the aggregate power consumption, the decoding threshold and the noise. By selecting a noise power density in {-169dBm/Hz,-171dBm/Hz,-173dBm/Hz} and a decoding threshold in $\{2, 2.5, 3, 3.5\}$, 12 simulation cases are performed. The aggregate power consumptions in the 12 cases for k=2 are listed in Table.II, and Table.III is for k=3. Note that all simulated cases are FSCs.

Based on Table.II and Table.III, we know that the higher is the noise power, the higher is the aggregate power consumption. Besides, the higher the decoding threshold, the higher the aggregate power consumption. Obviously, all of these conculsions are completely consistent.

TABLE. II. Aggregate power consumptions with k=2, L=15 and n=30

γ \ n_0	-169dBm/Hz	-171dBm/Hz	-173dBm/Hz
2	0.3935	0.2482	0.1566
2.5	0.5266	0.3323	0.2096
3	0.6737	0.4251	0.2682
3.5	0.8348	0.5267	0.3323

TABLE. III. Aggregate power consumption with k=3, L=10 and n=30

γ \ n_0	-169dBm/Hz	-171dBm/Hz	-173dBm/Hz
2	0.6334	0.3996	0.2521
2.5	0.9379	0.5918	0.3734
3	1.3184	0.8318	0.5248
3.5	1.7836	1.1254	0.7100

VII. Conclusions

Although SIC has a broad prospect for its support of real-time applications, its high power consumption is a major concern. The focus of this paper is the tradeoff between the power consumption and the real-time performance requirements of uplink transmissions in SIC-based wireless networks. Specifically, given the requirement of real-time performance, we aim to achieve the least aggregate power consumptions of UEs. We solve this problem by developing optimal power scheduling algorithms. Our conclusions are as follows. (1) The problem is solvable in $O(nlog(n))$ time in the case of continuous transmit power, and an optimal power scheduling strategy is obtained in this paper. (2) The requirement of real-time performance has a major impact on the power consumption than other factors, such as the number of simultaneous transmitters supported by SIC receiver. (3) With the optimal power scheduling strategy, SIC technology is suitable for low-power mobile applications because of the balanced power consumptions.

Appendix

A. A New Proof of Ordering Inequality

Ordering Inequality: Assume $a_1 \geq a_2 \geq \ldots \geq a_n$, $b_1 \leq b_2 \leq \ldots \leq a_n$, the optimal solution to the problem

$$\min_{X_{ij}} \sum_{i,j=1,\ldots,n} X_{ij} a_i b_j$$

$$s.t. \quad X_{ij} \in \{0,1\};$$

$$\sum_{i=1,\ldots,n} X_{ij} = 1 \ for\ all\ j \in [1,n]$$

$$\sum_{j=1,\ldots,n} X_{ij} = 1 \ for\ all\ i \in [1,n]$$

is $X_{ij} = \begin{cases} 1 & for\ all\ i = j \\ 0 & for\ all\ i \neq j \end{cases}$.

The ordering inequality is a well-known theorem, and we present a proof below for integrity.

It is easy to prove the case $n = 2$ since $a_1 b_1 + a_2 b_2 \geq a_1 b_2 + a_2 b_1$.

Assume that the assertion is true when $n = k - 1$.

For $n = k$, order that $\beta_i = b_i - b_1$ for all $i \in [2,k]$. We now only need to prove that $a_1 b_1 + a_2 (b_1 + \beta_2) + \ldots + a_k (b_1 + \beta_k) \leq b_1 a_{i1} + (b_1 + \beta_2) a_{i2} + \ldots + (b_1 + \beta_k) a_{ik}$, where $(a_{i1}, a_{i2}, \ldots, a_{ik})$ is any permutation of $\{a_1, a_2, \ldots, a_k\}$.

Case 1. $a_{i1} = a_1$. The assertion can be proved by the induction assumption of $n = k - 1$.

Case 2. $a_{i1} \neq a_1$. Since $(a_{i1}, a_{i2}, \ldots, a_{ik})$ is any permutation of $a_1, a_2, \ldots, a_k$, $a_{i1} + a_{i2} + \ldots + a_{ik} = a_1 + a_2 + \ldots + a_k$, and there exists a $j \in \{2, \ldots, k\}$, such that $a_{ij} = a_1$. Thus, $b_1 a_{i1} + (b_1 + \beta_2) a_{i2} + \ldots + (b_1 + \beta_k) a_{ik}$ = $b_1(a_1 + a_2 + \ldots + a_k) + \beta_2 a_{i2} + \beta_3 a_{i3} + \ldots + \beta_k a_{ik}$ = $b_1(a_1 + a_2 + \ldots + a_k) + \beta_2 a_{i2} + \beta_3 a_{i3} + \ldots + \beta_{j-1} a_{i(j-1)} + \beta_j a_1 + \beta_{j+1} a_{i(j+1)} + \ldots + \beta_k a_{ik} \geq b_1(a_1 + a_2 + \ldots + a_k) + \beta_2 a_{i2} + \beta_3 a_{i3} + \ldots + \beta_{j-1} a_{i(j-1)} + \beta_j a_{i1} + \beta_{j+1} a_{i(j+1)} + \ldots + \beta_k a_{ik}$.

Therefore, the case can be proved if $\beta_2 a_2 + \beta_3 a_3 + \ldots + \beta_k a_k \leq \beta_2 a_{i2} + \beta_3 a_{i3} + \ldots + \beta_{j-1} a_{i(j-1)} + \beta_j a_{i1} + \beta_{j+1} a_{i(j+1)} + \ldots + \beta_k a_{ik}$, which can be proved by the induction assumption for $\{a_1, a_2, \ldots, a_k\}$ and $\{\beta_1, \beta_2, \ldots, \beta_k\}$.

In conclusion, the assertion is proved.

B. Proof of Lemma 1

We prove the lemma by contradiction. W. l. o. g., we assume $G_1 < G_2 < \ldots < G_r$. In that case, we denote the descending order of channel gain as $\langle r, r-1, \ldots, 1 \rangle$, which means that signal of u_{i+1} is decoded prior to that of u_i.

Assume that the optimal decoding order is $D_1 = \langle s_r, s_{r-1}, \ldots, s_1 \rangle$ instead of $\langle r, r-1, \ldots, 1 \rangle$, and the optimal transmit powers for D_1 are $\{\overline{p}_{s_r}, \overline{p}_{s_{r-1}}, \ldots, \overline{p}_{s_1}\}$ for MPArPT, and $SINR_{s_l}^{D_1} \geq \gamma$ for all $l \in [1, r]$.

Assume that s_i is the first distinct element between $\langle s_r, s_{r-1}, \ldots, s_1 \rangle$ and $\langle r, r-1, \ldots, 1 \rangle$, i.e., $s_l = l$ for $\forall l \in [i+1, r]$ and $s_i < i$. There must exist an integer $j \in [1, i-1)$ such that $s_j = i$. Therefore, $G_{s_i} < G_{s_j}$, and $G_{s_i} \overline{p}_{s_i} > G_{s_j} \overline{p}_{s_j}$ if $\gamma > 1$, since signal of s_i is decoded before that of s_j.

Let $\widetilde{p}_{s_i} = \frac{G_{s_j} \overline{p}_{s_j}}{G_{s_i}}$ and $\widetilde{p}_{s_j} = \frac{G_{s_i} \overline{p}_{s_i}}{G_{s_j}}$. If we exchange s_i and s_j in D_1, we therefore get a new decoding order $D_2 = \langle r, r-1, \ldots, r-i, s_j, s_{i-1}, \ldots, s_{j+1}, s_i, s_{j-1}, \ldots, s_1 \rangle$. If the transmit powers for D_2 are set as $\langle \overline{p}_{s_r}, \overline{p}_{s_{r-1}}, \ldots, \overline{p}_{s_{r-i}}, \widetilde{p}_{s_j}, \overline{p}_{s_{i-1}}, \ldots, \overline{p}_{s_{j+1}}, \widetilde{p}_{s_i}, \overline{p}_{s_{j-1}}, \ldots, \overline{p}_{s_1} \rangle$, we have the following observations.

This article has been accepted for publication in a future issue of this journal, but has not been fully edited. Content may change prior to final publication. Citation information: DOI 10.1109/TVT.2017.2779784, IEEE Transactions on Vehicular Technology

(1) Constraint (2b) of MPArPT still holds, since

$$
\begin{aligned}
SINR_{s_j}^{D_2} &= \frac{G_{s_j}\widetilde{p}_{s_j}}{G_{s_i}\widetilde{p}_{s_i} + \sum\limits_{(\forall l\in[1,i-1])\cap(l\neq j)} G_{s_l}\overline{p}_{s_l} + n_0} \\
&= \frac{G_{s_i}\overline{p}_{s_i}}{\sum\limits_{\forall l\in[1,i-1]} G_{s_l}\overline{p}_{s_l} + n_0} \\
&= SINR_{s_i}^{D_1} \geq \gamma, \\
SINR_{s_i}^{D_2} &= \frac{G_{s_i}\widetilde{p}_{s_i}}{\sum\limits_{\forall l\in[1,j-1]} G_{s_l}\overline{p}_{s_l} + n_0} \\
&= \frac{G_{s_j}\overline{p}_{s_j}}{\sum\limits_{\forall l\in[1,j-1]} G_{s_l}\overline{p}_{s_l} + n_0} \\
&= SINR_{s_j}^{D_1} \geq \gamma, \\
SINR_{s_l}^{D_2} &= SINR_{s_l}^{D_1} \geq \gamma \quad \forall l \in [1,r], \quad l\neq i, \quad l \neq j.
\end{aligned}
$$

(2) Aggregate transmit power of D_2 is not larger than that of D_1. The reason can be explained by the fact that $\widetilde{p}_{s_i} + \widetilde{p}_{s_j} - \overline{p}_{s_i} - \overline{p}_{s_j} = \left(\frac{G_{s_j}-G_{s_i}}{G_{s_j}G_{s_i}}\right)\left(G_{s_j}\overline{p}_{s_j} - G_{s_i}\overline{p}_{s_i}\right) < 0$, and the transmit power of every other transmitter in D_1 is the same as that in D_2.

In all, D_2 is a better decoding order than D_1, which contradicts to the assumption that D_1 is the optimal decoding order. □

C. Proof of Theorem 1

It can be proved by mathematical induction as follows.

(1). $\widetilde{X}_1 \geq \widehat{X}_1$ because $\widetilde{X}_1 \geq \gamma n_0 = \widehat{X}_1$.

(2). Assume $\widetilde{X}_i \geq \widehat{X}_i \quad \forall i \in [1, l-1]$. Therefore $\widetilde{X}_l \geq \gamma\left(\sum\limits_{i=1}^{l-1}\widetilde{X}_i + n_0\right) \geq \gamma\left(\sum\limits_{i=1}^{l-1}\widehat{X}_i + n_0\right) = \widehat{X}_l$.

In conclusion, Theorem 1 is proved. □

D. Proof of Theorem 2

Since $\widehat{X}_r \geq \widehat{X}_{r-1} \geq \ldots \geq \widehat{X}_1$ and $G_1 \leq G_2 \leq \ldots \leq G_r$, based on the ordering inequality in Appendix.A, we know that $\sum\limits_{i=1}^{r}\frac{\widehat{X}_i}{G_i} \leq \sum\limits_{i=1}^{r}\frac{\widehat{X}_i}{G_i^{'}}$, where $\langle G_1^{'}, G_2^{'}, \ldots, G_r^{'}\rangle$ is any permutation of $\{G_1, G_2, \ldots, G_r\}$. On the other hand, for any solution $\left(\widetilde{X}_1, \widetilde{X}_2, \ldots, \widetilde{X}_r\right)$ to inequalities (4), since $\sum\limits_{i=1}^{r}\widehat{X}_i \leq \sum\limits_{i=1}^{r}\widetilde{X}_i$, $\sum\limits_{i=1}^{r}\frac{\widehat{X}_i}{G_i^{'}} \leq \sum\limits_{i=1}^{r}\frac{\widetilde{X}_i}{G_i^{'}}$. Therefore, $\sum\limits_{i=1}^{r}\frac{\widehat{X}_i}{G_i} \leq \sum\limits_{i=1}^{r}\frac{\widetilde{X}_i}{G_i^{'}}$. Note that $\left(\frac{\widehat{X}_1}{G_1}, \frac{\widehat{X}_2}{G_2}, \ldots, \frac{\widehat{X}_r}{G_r}\right)$ is a feasible solution to MPArPT, and $\left(\frac{\widetilde{X}_1}{G_1^{'}}, \frac{\widetilde{X}_2}{G_2^{'}}, \ldots, \frac{\widetilde{X}_r}{G_r^{'}}\right)$ is an arbitrary feasible solution to MPArPT, $\left(\frac{\widehat{X}_1}{G_1}, \frac{\widehat{X}_1}{G_2}, \ldots, \frac{\widehat{X}_r}{G_r}\right)$ is thus the optimal solution to MPArPT. □

E. Proof of Lemma 2

Based on the pigeonhole principle, for the optimal power scheduling strategy, assume there is a slot S_1 which has less than $\lfloor n/L \rfloor$ parallel UEs, there must exist another slot S_2 satisfying $|S_2| \geq 2 + |S_1|$, where $|S_1|$ is the cardinality of S_1. If the UE which is decoded first in S_2 is moved to S_1, a new power scheduling scheme will be formed. Based on Theorem 2, the aggregate power consumption of the new-formed scheduling strategy is less than that of the optimal one, which contradicts to the optimality.

Similarly, there could not be a slot which includes more than $\lceil n/L \rceil$ UEs. Therefore, the first statement of Lemma 2 is proved.

To prove the second statement, assume there are q slots each of which has $\lfloor n/L \rfloor$ users. Since $q\lfloor n/L\rfloor + (L-q)\lceil n/L \rceil = n$, $q = L\lceil n/L \rceil - n$ holds. □

F. Proof of Theorem 4

Our proof is based on the following facts.

(1). Based on the construction of $GH(n,k,L)$, and the mapping that the edge (u_i, T_{hj}) in $GH(n,k,L)$ means that u_i is scheduled in the hth slot, any feasible user scheduling strategy satisfying Lemma 2 can be mapped to a maximal matching of $GH(n,k,L)$, and vice versa. In other words, the mapping scheme is one-to-one.

(2). For the edge (u_i, T_{hj}) in $GH(n,k,L)$, $\widehat{X}_j/G_i$ is the minimum transmit power allocated to u_i if its decoding order index is j.

By taking them together, for any maximal matching of $GH(n,k,L)$, its weight sum is equal to nM minus the minimum aggregate power consumption of all UEs for the corresponding user scheduling strategy. So, the MWM of $GH(n,k,L)$ is the optimal solution to RMPS-kSIC, which is just what line 9 of Algorithm 1 does. □

G. Proof of Theorem 5

(1) Let $\{a_1, a_2, \ldots, a_n\} = \{\underbrace{\widehat{X}_{\lceil \frac{n}{L}\rceil}, \widehat{X}_{\lceil \frac{n}{L}\rceil}, \ldots, \widehat{X}_{\lceil \frac{n}{L}\rceil}}_{n-L\lfloor \frac{n}{L}\rfloor\ items}, \underbrace{\widehat{X}_{\lfloor \frac{n}{L}\rfloor}, \widehat{X}_{\lfloor \frac{n}{L}\rfloor}, \ldots, \widehat{X}_{\lfloor \frac{n}{L}\rfloor}}_{L\ items}, \ldots, \underbrace{\widehat{X}_2, \widehat{X}_2, \ldots, \widehat{X}_2}_{L\ items}, \underbrace{\widehat{X}_1, \widehat{X}_1, \ldots, \widehat{X}_1}_{L\ items}\}$ and $\{b_1, b_2, \ldots, b_n\} = \{\frac{1}{G_n}, \frac{1}{G_{n-1}}, \ldots, \frac{1}{G_1}\}$. For the following optimization problem (6), any of its feasible solution $\{X_{ij}, \forall i,j \in [1,n]\}$ corresponds to a matching of $GH(n,k,L)$. Further, the optimal solution to (6) corresponds to an MWM of $GH(n,k,L)$.

$$\min_{X_{ij}} \sum_{i,j=1..n} X_{ij}a_ib_j \tag{6a}$$

$$s.t. \quad X_{ij} \in \{0,1\}; \tag{6b}$$

$$\sum_{i=1..n} X_{ij} = 1 \ for\ all\ j \in [1,n] \tag{6c}$$

$$\sum_{j=1..n} X_{ij} = 1 \ for\ all\ i \in [1,n], \tag{6d}$$

(2) Based on the ordering inequality in Appendix.A, the optimal solution to (6) is also $\{X_{ij}\}$ where $X_{ij} = \begin{cases} 1 & for\ all\ i=j \\ 0 & for\ all\ i \neq j \end{cases}$. Besides, the output of Algorithm 2 also corresponds to the optimal solution to (6).

In summary, Algorithm 2 outputs the optimal solution to the RMPS-kSIC problem. □

H. Proof of Theorem 6

First, the MWM output by Algorithm 3 covers all real graph nodes. The assertion can be proved by a contradiction as follows.

Assume there is a real graph node u_i which is not covered by the MWM. If there is a virtual graph node v_j which is also not covered by the MWM, we can obtain another matching by adding (u_i, v_j) into the MWM. On the other side, if all virtual graph nodes have been covered in the MWM, there is at least one uncovered real graph node u_j besides u_i, because $2L - 2(2L - n)$ is an even number if $n > L$. Therefore, we can also obtain another matching by adding (u_i, u_j) into the MWM. In all, the assertion is proved.

Second, the output of Algorithm 3 is a feasible solution to RMDPS-2SIC, i.e., it satisfies all constraints of RMDPS-2SIC. Its proof is as follows.

(1) Since there are at most $2L$ graph nodes, its MWM includes at most L edges. Based on the mapping scheme, the frame length is thus at most L slots.

(2) Signal from every UE can be decoded correctly based on the power allocation mapped from MWM, which is from line 8 to line 16 in Algorithm 3. Besides, under the assumption that $\overline{tp}_m \geq \max_{(\forall i,j\in[1,n])\cap(i\neq j)} \max\left\{\left[\!\left[\frac{\gamma\left[\!\left[\frac{\widehat{X}_1}{G_i}\right]\!\right]G_i+\widehat{X}_1}{G_j}\right]\!\right], \left[\!\left[\frac{\gamma\left[\!\left[\frac{\widehat{X}_1}{G_j}\right]\!\right]G_j+\widehat{X}_1}{G_i}\right]\!\right]\right\}$, all transmit powers of UEs are in the set $\overline{TP}$.

(3) Every graph node will appear only once in a matching, and thus every UE has only one transmitting opportunity.

Third, the power scheduling strategy mapped from the output of Algorithm 3 achieves the minimum aggregate power consumption. Its proof is based on the following facts:

(1) For any maximal matching of GH, its weighted sum is nM minus the minimal aggregate transmit powers of all UEs.

(2) The Edmond's blossom algorithm finds an $MWM(GH)$ [27].

Put all these facts together, Algorithm 3 outputs an optimal solution to RMDPS-2SIC. □

I. Proof of Theorem 7

We prove it in two steps. In the first step, we consider the optimal power scheduling strategy of RMPS-kSIC for a given time slot, and w.l.o.g., assume $u_1, u_2, \ldots, u_k$ are in the given time slot and their channel gains are in the ascending order, i.e., $G_1 \leq G_2 \leq \ldots \leq G_k$.

If u_i is allocated with the discrete power $\widetilde{tp}_i$ by Algorithm 4[12], we assert that $\widetilde{tp}_i \leq \rho^i \left(\frac{G_i}{G_1}\right)^{i-1} \widehat{tp}_i$ holds for $\forall i \in [1, k]$. The assertion can be proved based on the following mathematical induction.

(1). $\widetilde{tp}_1 = \left[\!\left[\frac{\gamma n_0}{G_1}\right]\!\right] \leq \rho\widehat{tp}_1$.

(2). Assume for $\forall j \in [1, i-1], \widetilde{tp}_j \leq \rho^j \left(\frac{G_j}{G_1}\right)^{j-1} \widehat{tp}_j$ holds.

$$\widetilde{tp}_i = \left[\!\left[\frac{\gamma}{G_i}\left(n_0 + \sum_{j=1}^{i-1} \widetilde{tp}_j G_j\right)\right]\!\right] \quad \text{for} \quad \forall i \in [2, k],$$

$$\widetilde{tp}_i \leq \left[\!\left[\widehat{tp}_1 \tfrac{G_1}{G_i} + \gamma \sum_{j=1}^{i-1} \rho^j \left(\tfrac{G_j}{G_1}\right)^{j-1} \tfrac{G_j}{G_i}\widehat{tp}_j\right]\!\right] \leq \rho^i \left(\tfrac{G_i}{G_1}\right)^{i-2} \left(\widehat{tp}_1 \tfrac{G_1}{G_i} + \gamma \sum_{j=1}^{i-1} \tfrac{G_j}{G_i}\widehat{tp}_j\right) = \rho^i \left(\tfrac{G_i}{G_1}\right)^{i-2} \widehat{tp}_i \leq \rho^i \left(\tfrac{G_i}{G_1}\right)^{i-1} \widehat{tp}_i.$$

Therefore $\frac{\widetilde{tp}_i}{\widehat{tp}_i} \leq \rho^i \left(\frac{G_i}{G_1}\right)^{i-1}$ for $\forall i \in [1, k]$, thus the assertion is proved. So, $\frac{\sum_{i=1}^{k} \widetilde{tp}_i}{\sum_{i=1}^{k} \widehat{tp}_i} \leq \rho^k \left(\frac{G_k}{G_1}\right)^{k-1}$.

In the second step, based on Lemma 2 and Algorithm 2, the approximation ratio is $\frac{\sum_{i=1}^{n} \widetilde{tp}_i}{\sum_{i=1}^{n} \widehat{tp}_i} \leq$

$$\max\left\{\begin{array}{l} \rho^{\lfloor \frac{n}{L} \rfloor}\left(\max\limits_{i\in[(n\%L)+1,L]} \dfrac{G_{i+(\lfloor \frac{n}{L} \rfloor - 1)L}}{G_i}\right)^{\lfloor \frac{n}{L} \rfloor - 1}, \\ \rho^{\lceil \frac{n}{L} \rceil}\left(\max\limits_{i\in[1,n\%L]} \dfrac{G_{i+\lfloor \frac{n}{L} \rfloor L}}{G_i}\right)^{\lfloor \frac{n}{L} \rfloor} \end{array}\right\}.$$

If $\overline{tp}_m$ is no less than the maximum of the transmit powers allocated to UEs by Algorithm 4, the power scheduling strategy output by Algorithm 4 has the same user scheduling strategy output by Algorithm 1. Besides, note that the optimal aggregate transmit power of RMDPS-kSIC is no less than that of RMPS-kSIC. The approximation ratio of Algorithm 4 is thus no more than

$$\max\left\{\begin{array}{l} \rho^{\lfloor \frac{n}{L} \rfloor}\left(\max\limits_{i\in[(n\%L)+1,L]} \dfrac{G_{i+(\lfloor \frac{n}{L} \rfloor - 1)L}}{G_i}\right)^{\lfloor \frac{n}{L} \rfloor - 1}, \\ \rho^{\lceil \frac{n}{L} \rceil}\left(\max\limits_{i\in[1,n\%L]} \dfrac{G_{i+\lfloor \frac{n}{L} \rfloor L}}{G_i}\right)^{\lfloor \frac{n}{L} \rfloor} \end{array}\right\}. \quad \square$$

[12]For ease of presentation, we have some abuse on the notation $\widetilde{tp}$. Note that $\widetilde{tp}_i$ represents the power level allocated to u_i, while a two-dimension array is used in Algorithm 4.

References

[1] J. G. Andrews, S. Buzzi, W. Choi, S. V. Hanly, A. Lozano, A. C. K. Soong, and J. C. Zhang, "What will 5G be?" *IEEE J. Sel. Areas Commun.*, vol. 32, no. 6, pp. 1065–1082, Jun. 2014.

[2] F. Shan, W. Liang, J. Luo, and X. Shen, "Network lifetime maximization for time-sensitive data gathering in wireless sensor networks," *Comput. Netw.*, vol. 57, no. 5, pp. 1063–1077, 2013.

[3] Z. Yang, Z. Ding, P. Fan, and N. Al-Dhahir, "A general power allocation scheme to guarantee quality of service in downlink and uplink noma systems," *IEEE Trans. Wireless Commun.*, vol. 15, no. 11, pp. 7244–7257, Nov. 2016.

[4] L. Lei, D. Yuan, C. K. Ho, and S. Sun, "Power and channel allocation for non-orthogonal multiple access in 5g systems: Tractability and computation," *IEEE Trans. Wireless Commun.*, vol. 15, no. 12, pp. 8580–8594, Dec. 2016.

[5] Z. Wei, D. W. K. Ng, and J. Yuan, "Power-efficient resource allocation for mc-noma with statistical channel state information," in *Proc. 59th IEEE GLOBECOM*, Washington, DC, USA, Dec. 2016, pp. 1–7.

[6] X. Zhang and M. Haenggi, "The performance of successive interference cancellation in random wireless networks," *IEEE Trans. Inf. Theory*, vol. 60, no. 10, pp. 6368–6388, Oct. 2014.

[7] L. Kong and X. Liu, "mzig: Enabling multi-packet reception in zigbee," in *Proc. 21st ACM MOBICOM*, New York, NY, USA, Sep. 2015, pp. 552–565.

[8] D. Halperin, T. Anderson, and D. Wetherall, "Taking the sting out of carrier sense: Interference cancellation for Wireless LANs," in *Proc. 14th ACM MOBICOM*, New York, NY, USA, Sep. 2008, pp. 339–350.

[9] S. Sen, N. Santhapuri, R. R. Choudhury, and S. Nelakuditi, "Successive interference cancellation: Carving out MAC layer opportunities," *IEEE Trans. Mobile Comput.*, vol. 12, no. 2, pp. 346–357, Feb. 2013.

[10] C. Jiang, Y. Shi, X. Qin, X. Yuan, Y. T. Hou, W. Lou, S. Kompella, and S. F. Midkiff, "Cross-layer optimization for multi-hop wireless networks with successive interference cancellation," *IEEE Trans. Wireless Commun.*, vol. 15, no. 8, pp. 5819–5831, Aug. 2016.

[11] E. Karipidis, D. Yuan, Q. He, and E. G. Larsson, "Max-min power control in wireless networks with successive interference cancelation," *IEEE Trans. Wireless Commun.*, vol. 14, no. 11, pp. 6269–6282, Nov. 2015.

[12] D. Yuan, V. Angelakis, L. Chen, E. Karipidis, and E. G. Larsson, "On optimal link activation with interference cancelation in wireless networking," *IEEE Trans. Veh. Technol.*, vol. 62, no. 2, pp. 939–945, Feb. 2013.

[13] L. Qu, J. He, and C. Assi, "Understanding the benefits of successive interference cancellation in multi-rate multi-hop wireless networks," in *Proc. IEEE ICC 2014*, Sydney, Australia, Jun. 2014, pp. 354–360.

[14] C. Xu, L. Ping, P. Wang, S. Chan, and X. Lin, "Decentralized power control for random access with successive interference cancellation," *IEEE J. Sel. Areas Commun.*, vol. 31, no. 11, pp. 2387–2396, Nov. 2013.

[15] O. Goussevskaia and R. Wattenhofer, "Scheduling with interference decoding: Complexity and algorithms," *Ad Hoc Netw.*, vol. 11, no. 6, pp. 1732–1745, Aug. 2013.

[16] S. Lv, W. Zhuang, M. Xu, X. Wang, C. Liu, and X. Zhou, "Understanding the scheduling performance in wireless networks with successive interference cancellation," *IEEE Trans. Mobile Comput.*, vol. 12, no. 8, pp. 1625–1639, Aug. 2013.

[17] A. Sankararaman and F. Baccelli, "CSMA k-SIC - A class of distributed mac protocols and their performance evaluation," in *Proc. 34th IEEE INFOCOM*, Hong Kong, China, Apr. 2015, pp. 2002–2010.

[18] Z. Ding, P. Fan, and H. V. Poor, "Impact of user pairing on 5G nonorthogonal multiple-access downlink transmissions," *IEEE Trans. Veh. Technol.*, vol. 65, no. 8, pp. 6010–6023, Aug. 2016.

[19] Z. Yang, Z. Ding, P. Fan, and N. Al-Dhahir, "A general power allocation scheme to guarantee quality of service in downlink and uplink noma systems," *IEEE Trans. Wireless Commun.*, vol. 15, no. 11, pp. 7244–7257, Nov. 2016.

[20] M. Mollanoori and M. Ghaderi, "Uplink scheduling in wireless networks with successive interference cancellation," *IEEE Trans. Mobile Comput.*, vol. 13, no. 5, pp. 1132–1144, May 2014.

[21] C. W. Sung and Y. Fu, "A game-theoretic analysis of uplink power control for a non-orthogonal multiple access system with two interfering cells," in *Proc. 83rd IEEE VTC*, Nanjing, China, May 2016, pp. 1–5.

[22] L. P. Qian, Y. Wu, H. Zhou, and X. Shen, "Joint uplink base station association and power control for small-cell networks with non-orthogonal multiple access," *IEEE Trans. Wireless Commun.*, vol. 16, no. 9, pp. 5567–5582, Sep. 2017.

[23] B. Wang, L. Dai, Y. Yuan, and Z. Wang, "Compressive sensing based multi-user detection for uplink grant-free non-orthogonal multiple access," in *Proc. 82nd IEEE VTC*, Boston, USA, Sep. 2015, pp. 1–5.

[24] C. Xu, H. Ding, and Y. Xu, "Low-complexity uplink scheduling algorithms with power control in successive interference cancellation based wireless mud-logging systems," *Wireless Netw.*, no. 3, pp. 1–14, Jul. 2017. DOI=https://doi.org/10.1007/s11276-017-1561-7.

[25] D. B. Green and A. S. Obaidat, "An accurate line of sight propagation performance model for ad-hoc 802.11 Wireless LAN (WLAN) devices," in *Proc. IEEE ICC 2002*, vol. 5, Apr. 2002, pp. 3424–3428.

[26] J. R. Barry, E. A. Lee, and D. G. Messerschmitt, *Digital Communication, 3rd ed.* Springer-Verlag, Sep. 2003.

[27] V. Kolmogorov, "Blossom V: a new implementation of a minimum cost perfect matching algorithm," *Mathematical Programming Computation*, vol. 1, no. 1, pp. 43–67, Jul. 2009.

Chaonong Xu received his B.S. and M.S. degrees in computer sciences from Hefei University of Technology, China, in 1998 and 2001, and his Ph. D. degree in computer science from the Institute of Computing Technology, Chinese Academy of Sciences in 2007, respectively. He joined Tsinghua University as a postdoctor in 2007. He is now an associate professor in China University of Petroleum, Beijing, China. His research interests cover embedded system and wireless networks.

Kaichi Ma received his B.S. degree from China University of Petroleum, Beijing in 2015. He is now a M.S. candidate in the Department of Computer Science and Technology, China University of Petroleum, Beijing. His research interests cover wireless communication and networks.

Yida Xu received his B.S. degree from University of Science and Technology of China in 2011, and M.S. degree in 2017 from China University of Petroleum, Beijing. He is now a Ph.D. candidate in the Institute of Computing Technology, Chinese Academy of Sciences. His research interests cover wireless communication and networks.

Yongjun Xu received his B.S. degree in 2001 from Xi'an University of Posts and Telecommunications, China, and Ph.D. degree from the Institute of Computing Technology, Chinese Academy of Sciences in 2006. He is now an associate professor at the Institute of Computing Technology, Chinese Academy of Sciences. His research interests cover low power system and wireless sensor networks.

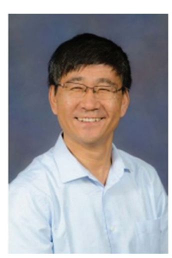

Yuguang Fang (F'08) received the M.S. degree from Qufu Normal University, Shandong, China, in 1987, the Ph.D. degree from Case Western Reserve University, in 1994, and the Ph.D. degree from Boston University, in 1997. He joined the Department of Electrical and Computer Engineering, University of Florida, in 2000, and has been a full professor since 2005. He held a University of Florida Research Foundation Professorship (2006-2009), a Changjiang Scholar Chair Professorship with Xidian University, China (2008-2011) and with Dalian Maritime University (2015-present), and a Guest Chair Professorship with Tsinghua University, China, from (2009-2012). He was the editor-in-chief of the IEEE Transactions on Vehicular Technology (2013-2017), was the editor-in-chief of the IEEE Wireless Communications (2009-2012). He is a fellow of the IEEE and the AAAS.